*J. Phys. Chem. A* **1997,** *101,* 2715−2722

# Molecular Orbital Calculation of $^{27}$Al and $^{29}$Si NMR Parameters in $Q^3$ and $Q^4$ Aluminosilicate Molecules and Implications for the Interpretation of Hydrous Aluminosilicate Glass NMR Spectra

**Dan Sykes,*,† J. D. Kubicki,‡,§ and Thomas C. Farrar†,||**

*Department of Chemistry, 1101 University Avenue, University of Wisconsin—Madison,*
*Madison, Wisconsin 53706, Remediation Research Laboratory, Chemistry and Biochemistry Branch,*
*Naval Command, Control, and Ocean Surveillance Center, RDT&E Division, Code D361,*
*San Diego, California 92152-6325*

*Received: November 21, 1996*⊗

The basis set dependency of Al and Si isotropic chemical shieldings in $Al^{3+}\cdot 6(H_2O)$, $[Al(OH)_4]^{1-}\cdot 2(H_2O)$, and tetramethylsilane have been calculated using the GIAO formalism. The Si chemical shielding changes substantially with the addition of extra d-functions; however, this influence is smaller than the effect of using a 311 split valence shell representation. Similarly, the addition of a second set of d-functions to Al lowers the chemical shielding; however, the addition of extra d-functions does not affect the chemical shielding as much if the triply-split valence shell representation is used. The 6-31G* calculation predicts accurate *relative chemical shifts* for the tetrahedral Al molecule $[Al(OH)_4]^{1-}\cdot 2(H_2O)$ nearest to the experimental value of 79.9 ppm. Calculations were also performed on large (∼20 heavy atoms) aluminosilicate molecules to test peak assignments in the experimental NMR spectra of anhydrous and hydrous aluminosilicate glasses.

## 1. Introduction

$^{27}$Al and $^{29}$Si nuclear magnetic resonance (NMR) spectroscopies have been employed extensively in the study of the structures and dynamics of aqueous-phase species in groundwater and soil pore waters, aluminosilicate-based glasses, zeolites and xerogels, and minerals. For most of these materials, it is difficult to obtain unambiguous structural information beyond an empirical interpretation of the spectra. Assignment of peaks in the NMR spectra of these nuclei are typically based on the behavior of line shapes as composition is varied or by analogy with related compounds with known structures. For example, glass NMR spectra are often interpreted in terms of the crystal spectra of the same composition, but this is not always possible, as in the case of hydrous aluminosilicate glasses.

Water solubility mechanisms in aluminosilicate glasses and melts have been the subject of recent debate.[1−3] In the Raman and IR spectra of hydrous glasses, a band near 880 cm$^{-1}$ appears that is not present in spectra of the anhydrous glasses.[3−6] The NMR spectra of hydrous sodium aluminosilicate glasses are characterized by slightly smaller $^{29}$Si chemical shifts, slightly greater $^{27}$Al chemical shifts and narrower line widths, and a significant increase in the quadrupolar coupling constant of $^{23}$Na above approximately 30 mol% $H_2O$.[1ab,2a] Kohn et al.[1ab] and Pichavant et al.[2] interpret the changes in the Raman and NMR spectra to be consistent with protonation of some of the bridging oxygens in Al−O−Al and Al−O−Si linkages to form Al−($O_{br}$H)−Al, Al−($O_{br}$H)−Si and $Na(OH)_m(H_2O)_n$ complexes. Sykes and Kubicki[3] interpret the same spectra to be the result of hydrolysis of Al−O−Si and Al−O−Al linkages to form terminal Al−(OH) and Si−(OH) bonds. In this model, $Na(OH)_m(H_2O)_n$ complexes form for total water contents greater than 30 mol%.

Because of the ambiguity in the interpretation of the spectra, it is important to have a means by which assignments can be tested in an objective and quantitative manner. *Ab initio* molecular orbital calculations have proven to be a reliable means for testing interpretations of NMR and vibrational spectra of organic species and to some extent small silicate species. In an attempt to test the proposed NMR peak assignments of hydrous and anhydrous albite composition glasses ($NaAlSi_3O_8$−$H_2O$), Al NMR parameters (isotropic chemical shieldings, isotropic chemical shifts, and quadrupolar coupling constants) were calculated for the optimized geometries of the molecules $[((OH)_3SiO)_3Al{-}(OH)]^{1-}$, $[((OH)_3Si)_4AlO_4]^{1-}$, $Na[((OH)_3SiO)_3{-}Al{-}(OH)]$, $Na[((OH)_3Si)_4AlO_4]$, $Na[((OH)_3Si)_3((OH)_3Al)AlO_4]^{1-}$, $[((OH)_3Si)_4(OH)AlO_3]$, $Na[((OH)_3SiO)_2((OH)_3AlO)Si{-}(OH)]$, $Na[((OH)_3Si)_3((OH)_3Al)SiO_4]$, and $[((OH)_3Si)_3((OH)_3Al)(OH){-}SiO_4]$, which represent proposed species in each of the models.

We have also calculated the basis set dependency of the isotropic chemical shielding values for Al in $Al^{3+}\cdot 6(H_2O)$ and isotropic chemical shift values for Al in $[Al(OH)_4]^{1-}\cdot 2(H_2O)$. In a previous study,[7] we have demonstrated that progressive deprotonation of the $Al^{3+}\cdot 6(H_2O)$ molecule accurately models the experimental deprotonation trend and predicts the octahedral to tetrahedral coordination change of Al in this series. The 79.9 ppm chemical shift of the aqueous $[Al(OH)_4]^{1-}\cdot 2(H_2O)$ species is used as an internal standard for experimental NMR investigations of aqueous-phase Al species and is used here as a measure of the accuracy of the chemical shift calculations for the theoretical $[Al(OH)_4]^{1-}\cdot 2(H_2O)$ molecule.

There is general agreement that the appearance of the peaks near 970 cm$^{-1}$ in the Raman and IR spectra and −100 and −90 ppm in the $^{29}$Si NMR spectra of hydrous silica glasses, which are absent in the anhydrous glass spectra, are indicative of the hydrolysis of Si−O−Si → Si−OH.[5,8] As a test of the accuracy of the chemical shift calculations and relevance of these gas-phase models to glass spectra, we have determined the basis set dependency of the Si chemical shielding value for TMS and

---

* Author to whom correspondence should be addressed: E-mail, dan@chem.wisc.edu.
† Department of Chemistry.
‡ Remediation Research Laboratory.
§ kubicki@nosc.mil.
|| dan@chem.wisc.edu.
⊗ Abstract published in *Advance ACS Abstracts,* March 15, 1997.

S1089-5639(96)03891-1 CCC: $14.00

**TABLE 1: Theoretical Molecules, $Q^n$ Designations, and Representative $Q^n$ Species in Anhydrous and Hydrous Aluminosilicate Glasses. Silica = $SiO_2$ Glass; Albite = $NaAlSi_3O_8$ Glass**

| molecule | $Q^n$ label | $Q^n$ species in glass |
|---|---|---|
| $[((OH)_3SiO)_4Si]$ | $Q^4$Si | $Q^4$Si in anhydrous silica |
| $[((OH)_3SiO)_3Si(OH)]$ | $Q^3$Si | $Q^3$Si−(OH) in hydrous silica |
| $[((OH)_3SiO)_2Si{-}(OH)_2]$ | $Q^2$Si | $Q^2$Si−(OH) in hydrous silica |
| $Na[((OH)_3Si)_3((OH)_3Al)SiO_4]$ | $Q^4$Si (Al,Na) | $Q^4$Si in anhydrous albite |
| $Na[((OH)_3SiO)_2(OH)_3AlO)Si(OH)]$ | $Q^3$Si (Al,Na) | $Q^3$Si−(OH) in hydrous albite |
| $H[((OH)_3SiO)_3((OH)_3AlO)SiO_4]$ | $Q^4$Si (Al−$O_{br}$H) | $Q^4$Si in hydrous albite[a] |
| $[((OH)_3SiO)_4Al]^{1-}$ | $Q^4$Al | $Q^4$Al in anhydrous albite |
| $Na[((OH)_3SiO)_4Al]$ | $Q^4$Al (Na) | $Q^4$Al in anhydrous albite |
| $Na[((OH)_3SiO)_3((OH)_3AlO)Al]^{1-}$ | $Q^4$Al (Al,Na) | $Q^4$Al in anhydrous albite |
| $[((OH)_3SiO)_3Al(OH)]^{1-}$ | $Q^3$Al | $Q^3$Al−(OH) in hydrous albite |
| $Na[((OH)_3SiO)_3Al(OH)]$ | $Q^3$Al (Na) | $Q^3$Al−(OH) in hydrous albite |
| $[((OH)_3Si)_4(OH)AlO_3]$ | $Q^4$Al ($O_{br}$H) | $Q^4$Al in hydrous albite[a] |

[a] $Q^4$ species with protonated bridging oxygen as proposed by Kohn et al.[1b] and Pichavant et al.[2]

calculated Si chemical shifts for the molecules $[((OH)_3Si)_4SiO_4]$, $[((OH)_3SiO)_3Si{-}(OH)]$, and $[((OH)_3SiO)_2Si{-}(OH)_2]$ to compare with the NMR spectra of anhydrous and hydrous silica glass.

The basis set dependency of the absolute chemical shielding value for Si in tetramethyl silane (TMS), the experimental NMR standard for $^{29}$Si nuclei, has been calculated previously.[9−11] To the best of our knowledge, a systematic investigation of the basis set dependency of the chemical shielding values for Al in $Al^{3+}{\cdot}6(H_2O)$, the experimental NMR standard for $^{27}$Al nuclei, has not been conducted.

## 2. Methods

**2.1. Geometry Optimization.** Calculations were performed with GAUSSIAN 94.[12] Minimum potential energy structures for the molecules $Al^{3+}{\cdot}6(H_2O)$ and $[Al(OH)_4]^{1-}{\cdot}2(H_2O)$ were calculated using self-consistent, Hartree−Fock molecular orbital calculations with 3-21G**, 6-31G*, and 6-311+G** basis sets. Geometry optimizations were also performed using Møller−Plesset second-order perturbation theory (MP2) with the 6-311+G** basis on selected molecules. Because of the large size of the aluminosilicate molecules, geometry optimizations were performed using only the 3-21G** basis set. No symmetry constraints were placed on any of the molecules; redundant internal coordinates[13] of each molecule were varied to allow for full optimizations. Potential energy minima were located with the Berny optimization algorithm.[14,15] Stationary points were found to be true minima of the molecular potential energy surface through force constant analyses; however, we make no claim that the structures represent global minima on the potential energy surface.

At a minimum in the potential energy surface of a molecule, first derivatives of atomic displacements will be equal to zero (*i.e.*, $(dV/dr) = 0$, where $V$ is the potential energy and $r$ is an atomic coordinate) and all second derivatives are positive (*i.e.*, $(d^2V/dr^2) > 0$). Harmonic expansion of the interatomic potential then provides an estimate of vibrational frequencies. Force constant analyses of the optimized geometries based on diagonalization of the Hessian matrix (*i.e.*, the second derivatives of the potential energy surface) were carried out for all clusters. No imaginary frequencies were found for the structures.

**2.2. Chemical Shielding ($\sigma$) and Quadrupolar Coupling Constants.** Calculations were performed using gauge-including atomic orbitals (GIAO) as implemented in Texas 90, Texas 93,[16] and Gaussian 94.[16−20] The GIAO algorithm computes chemical shieldings for nuclei based on finite perturbation theory which involves solving for the second derivative of the energy with respect to the magnetic field and the magnetic moment of the nucleus. Using the GIAO formalism, the chemical shielding cannot be separated into the diamagnetic and paramagnetic contributions of the Ramsey equations. The isotropic chemical shielding $\sigma_{iso}$ is obtained by averaging the three principal tensor components of the chemical shielding, $\sigma_{xx}$, $\sigma_{xx}$, and $\sigma_{zz}$. Isotropic chemical shifts $\delta_{iso}$ were calculated using the formula $\delta_{iso} = \sigma_{iso}{}^{ref} - \sigma_{iso}{}^{molecule}$, where $\sigma_{iso}{}^{ref}$ is either the chemical shielding value for Al in $Al^{3+}{\cdot}6(H_2O)$ or Si in TMS.

Quadrupolar coupling constants (QCC) and asymmetry parameters $\eta$ were calculated using $QCC = eq_{zz}eQ$ and $\eta = |q_{xx} - q_{yy}/q_{zz}|$ where $eQ$ is the nuclear electric quadrupole moment of the nucleus and all other terms are the principal tensor components of the electric field gradient (EFG). The isotropic chemical shieldings, quadrupolar coupling constants, and asymmetry parameters were calculated using RHF/3-21G**, 6-31G*, 6-31+G*, 6-31G(2d), 6-311+G**, 6-311+G(3df,2p) basis sets.

## 3. Results and Discussion

**3.1. Optimized Geometries of the Standards.** Table 1 lists the molecules investigated in this study and the molecular species each represents in anhydrous and hydrous aluminosilicate melts and glasses. In the zeolite and melt/glass literature, tetrahedral aluminosilicate species are typically designated as $Q^n$ species where Q is the central tetrahedral cation (Al or Si) and $n$ is the number of oxygens that bridge ($O_{br}$) the central cation to other tetrahedral Al or Si sites. For example, the $Q^4$-Al species is a tetrahedral Al with all four oxygens connecting the central Al tetrahedron to four Si tetrahedra. Similarly, the $Q^4$Al (Al,Na) species has four $O_{br}$ connecting the central Al tetrahedron to four other tetrahedra, one of which is an aluminate tetrahedron. The $Na^+$ is a nonframework cation. The $Q^4$Al and $Q^4$Al (Al,Na) molecules have a −1 charge, whereas the $Q^4$Al(Na) molecule is electrically neutral. The central tetrahedral nuclei in all $Q^3$ species have three $O_{br}$ and one terminal −(OH) group and represent the products of the hydrolysis reaction Al−O−Al, Si−O−Al, or Si−O−Si → Al−OH, and/or Si−OH (*i.e.*, $Q^4 \rightarrow Q^3$). The $Q^4$Si (Al−$O_{br}$H) and $Q^4$Al ($O_{br}$H) represent the products of the reaction Si−O−Al → Si−($O_{br}$H)−Al (*i.e.*, $Q^4 \rightarrow Q^4$ ($O_{br}$H)), in which one of the bridging oxygens is protonated.

The 3-21G** optimized geometries for the TMS, $Al^{3+}{\cdot}6(H_2O)$, and $[Al(OH)_4]^{1-}{\cdot}2(H_2O)$ molecules are given in Figure 1. The TMS molecule optimized to $T_d$ symmetry with intertetrahedral CSiC angles of 109.5°. The average Si−C and C−H bond lengths of 1.890 and 1.085 Å, respectively, are consistent with experimental values and represent typical bond lengths for methylated silanes.[11,21,22]

The $Al^{3+}{\cdot}6(H_2O)$ complex is a regular octahedral configuration with Al−O bond distances of 1.912 Å, comparable to an average Al−O of 1.93 Å in solids.[23] The $[Al(OH)_4]^{1-}{\cdot}2(H_2O)$

**TABLE 2: 3-21G** Optimized Geometries for the Aluminosilicate Molecules. Distances Angstroms and Angles are in Degrees. Numbers in broken brackets (⟨ ⟩) are Average Values**

| molecule | Si−$O_{br}$ | Si−$O_{nbr}$ | Al−$O_{br}$ | Al−$O_{nbr}$ | T−(OH) | O−H | SiOSi | SiOAl | AlOAl |
|---|---|---|---|---|---|---|---|---|---|
| $Q^2$Si | ⟨1.619⟩ | ⟨1.623⟩ | | | ⟨1.612⟩ | ⟨0.939⟩ | 144.0 | | |
| $Q^3$Si | ⟨1.610⟩ | ⟨1.620⟩ | | | 1.633 | ⟨0.937⟩ | ⟨147.0⟩ | | |
| $Q^4$Si | ⟨1.611⟩ | ⟨1.621⟩ | | | | ⟨0.939⟩ | ⟨158.7⟩ | | |
| $Q^3$Si (Al,Na) | ⟨1.612⟩ | ⟨1.626⟩ | 1.789 | ⟨1.740⟩ | 1.622 | ⟨0.938⟩ | ⟨158.2⟩ | 141.3 | |
| $Q^4$Si (Al,Na( | ⟨1.617⟩ | ⟨1.626⟩ | 1.758 | ⟨1.748⟩ | | ⟨0.942⟩ | ⟨146.5⟩ | 148.9 | |
| $Q^4$Si (Al−$O_{br}$H) | ⟨1.623⟩ | ⟨1.621⟩ | 1.888 | ⟨1.714⟩ | | ⟨0.943⟩ | ⟨146.6⟩ | 122.4 | |
| $Q^3$Al | ⟨1.607⟩ | ⟨1.634⟩ | ⟨1.740⟩ | | 1.779 | ⟨0.939⟩ | | ⟨133.8⟩ | |
| $Q^4$Al | ⟨1.600⟩ | ⟨1.638⟩ | ⟨1.740⟩ | | | ⟨0.944⟩ | | ⟨131.1⟩ | |
| $Q^3$Al (Na) | ⟨1.595⟩ | ⟨1.636⟩ | ⟨1.747⟩ | | 1.737 | ⟨0.941⟩ | | ⟨147.6⟩ | |
| $Q^4$Al (Na) | ⟨1.594⟩ | ⟨1.640⟩ | ⟨1.742⟩ | | | ⟨0.942⟩ | | ⟨137.5⟩ | |
| $Q^4$Al (Al,Na) | ⟨1.594⟩ | ⟨1.642⟩ | ⟨1.745⟩ | ⟨1.769⟩ | | ⟨0.946⟩ | | ⟨145.7⟩ | 130.8 |
| $Q^4$Al ($O_{br}$H) | ⟨1.632⟩ | ⟨1.626⟩ | ⟨1.746⟩ | | | ⟨0.943⟩ | | ⟨135.2⟩ | |

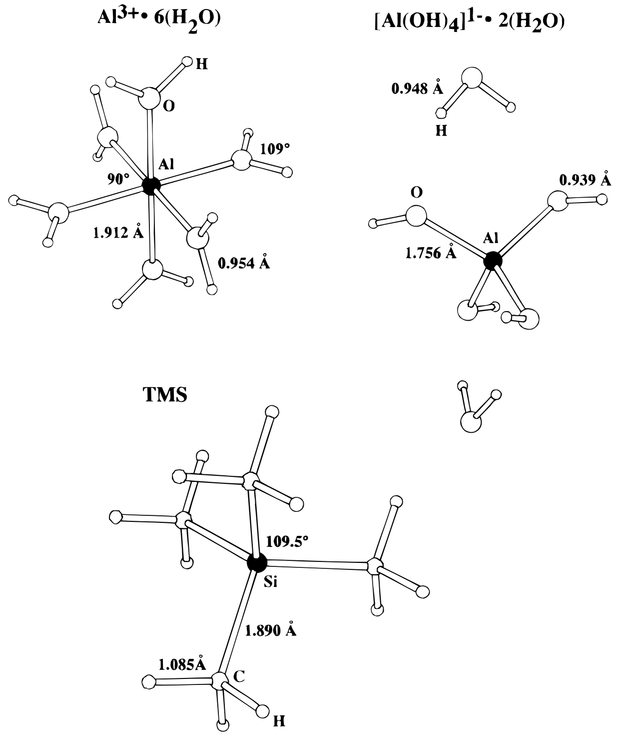

**Figure 1.** Optimized geometries (HF/3-21G**) of the Al and Si reference molecules.

complex is a tetrahedral configuration with Al−(OH) bonds near 1.76 Å comparable to an average Al−O distance of 1.77 Å for tetrahedral $Al^{3+}$ in solids.[23] The Al−($OH_2$) distances are near 3.42 Å. Structural parameters of fully optimized geometries obtained using HF/6-311+G** and MP2/6-311+G** basis sets change by less than 2% from the 3-21G** optimized complexes. A more complete discussion of the structures of these two molecules can be found elsewhere.[7]

**3.2. Optimized Geometries of the Aluminosilicate Molecules.** The 3-21G** optimized geometries for the aluminosilicate molecules are given in Table 2 and Figures 2−4. Calculated T−O bond distances and TOT angles for all aluminosilicate molecules are comparable to previous experimental and theoretical studies of T−O bond distances and TOT angles in glass and crystalline aluminosilicates.[3c,24−30] The average Si−O−Si and Si−O−Al angles are similar to those found in silica and sodium aluminosilicate glasses (144° and 138°, respectively)[31,32] and the range of intertetrahedral angles coincides with the observed range of 120°−180°.[33] In general, T−$O_{br}$, T−$O_{nbr}$ and O−H bond lengths change by less than 1% between $Q^3$ and $Q^4$ species and between neutral and negatively charged molecules for a given $Q^n$ species. The exceptions are the protonated T−($O_{br}$H) bond lengths in the $Q^4$ ($O_{br}$H) species. The Si−($O_{br}$H) and Al−($O_{br}$H) bond lengths of 1.719 and 1.861 Å, respectively, are over 0.1 Å larger than the Si−$O_{br}$ and Al−$O_{br}$ for the unprotonated T−O−T linkages in the $Q^4$ ($O_{br}$H) molecules and in all other molecules. The Si−($O_{br}$H) and Al−($O_{br}$H) bond lengths are near the 1.76 Å $Si^{VI}$−O distance in stishovite[34] and the 1.86 and 1.97 Å $Al^{VI}$−O distances in corundum.[35] Concurrent with this bond lengthening due to protonation of the Si−O−Al linkages is a narrowing of the Si−O−Al angles by 22° and 13° for the $Q^4$Al ($O_{br}$H) and $Q^4$Si (Al−$O_{br}$H) molecules, respectively.

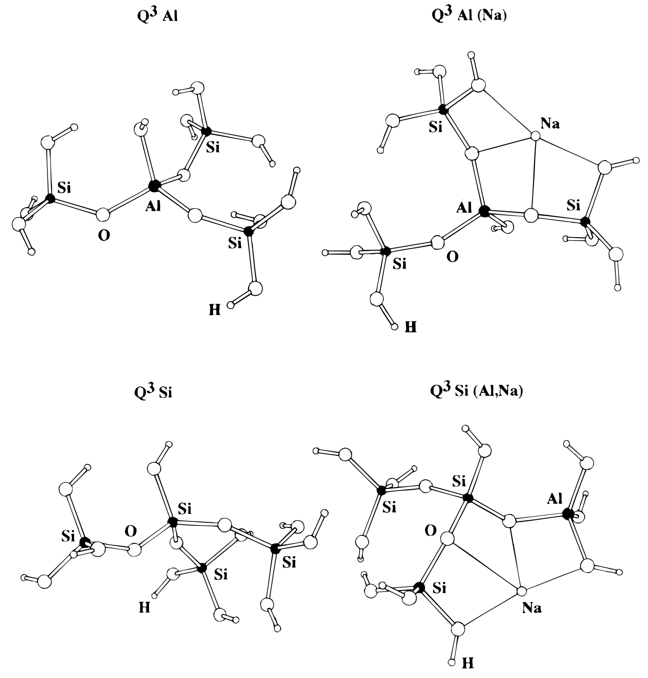

**Figure 2.** Optimized geometries (HF/3-21G**) of the $Q^3$Al and Si molecules.

**3.3. Si Isotropic Chemical Shieldings and Shifts.** The GIAO calculations performed using 6-31G*, 6-31G(2d), 6-311+G**, 6-31G(3df,2p), and 6-311+G(3df,2p) basis sets predict isotropic chemical shielding values for Si in the TMS molecule of 450, 432, 397, 419, 381 ppm, respectively (Table 3). These values approach the absolute chemical shielding values of 368.5, 375.1, and 379.5 ppm obtained by Jameson and Jameson[9], Kutzelnigg et al.,[10] and Wolff and Radeglia,[11] respectively. The chemical shielding changes substantially with the addition of extra d-functions on Si; however, this influence is smaller than the effect of using the 311 split valence shell representation and the addition of the diffuse functions. Previous studies have noted that a single set of d-functions are sufficient for small Si compounds,[10,36] but the large size of the TMS and aluminosilicate molecules in the present study most

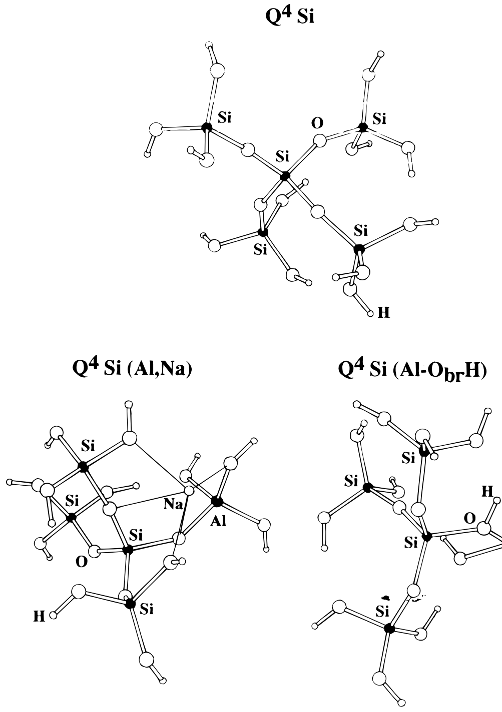
$Q^4$ Si

$Q^4$ Si (Al,Na)

$Q^4$ Si (Al-$O_{br}$H)

**Figure 3.** Optimized geometries (HF/3-21G**) of the $Q^4$Si molecules.

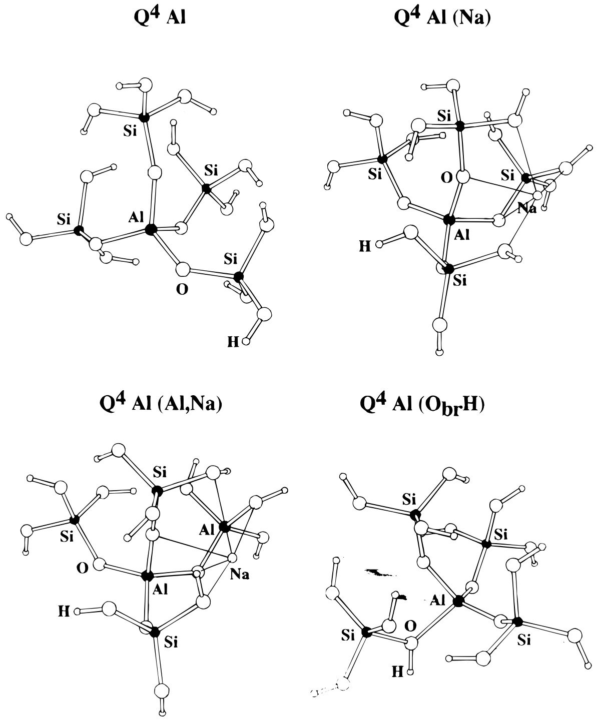
$Q^4$ Al

$Q^4$ Al (Na)

$Q^4$ Al (Al,Na)

$Q^4$ Al ($O_{br}$H)

**Figure 4.** Optimized geometries (HF/3-21G**) of the $Q^4$Al molecules.

likely require both split valence shell representations and three sets of d-functions to obtain shielding values near 375 ppm.

The calculated isotropic chemical shieldings for the $Q^2$Si, $Q^3$Si, and $Q^4$Si molecules also depend on the basis set. As with TMS, predicted chemical-shielding values decrease from the 6-31G* calculation to the 6-311+G** calculation (Table 3). In contrast, however, calculated chemical shifts are less sensitive to the number of d-functions used in a given basis set. In the present study, only the chemical shifts, relative to TMS, calculated for the $Q^2$Si (−87 ppm), $Q^3$Si (−98 ppm), and the $Q^4$Si (−112 ppm) using 6-311+G** (Table 3) are comparable to the experimental values of −91 ppm, −100 ppm, and −112 ppm, respectively, observed in hydrous and anhydrous silica glass $^{29}$Si NMR spectra.[8] The 6-31G* and 6-31G(2d) basis sets predict chemical shifts, relative to TMS, approximately 15 ppm smaller than the experimentally measured $^{29}$Si shifts of their natural analog compositions. However, the predicted chemical shift differences *between* $Q^2$, $Q^3$, and $Q^4$Si species with a given basis set are similar to the experimentally measured differences. For example, the measured difference between $Q^3$ and $Q^4$ in silica and hydrous silica glasses is 12 ppm, and the calculated difference between $Q^3$ and $Q^4$ with the 6-31G* and 6-31G(2d) basis sets are 7 and 11 ppm, respectively (Table 3). We note that, for almost all basis sets, chemical shieldings and chemical shifts for the $Q^3$Si molecules are more positive (*i.e.*, less shielded) than the shielding values for the corresponding $Q^4$Si molecules. In contrast, the chemical shielding and chemical shift values for the $Q^4$Si (Al,Na) molecule are more positive than the values for the $Q^3$Si (Al,Na) molecule for all basis sets. Experimental $^{29}$Si NMR spectra exhibit a progressive deshielding of the Si nuclei as the number of $O_{br}$ decreases, $Q^4 \rightarrow Q^0$.[37−39] This discrepancy between theory and experiment likely arises from our underestimate of the $^{29}$Si chemical shift in albite glass; the experimental $^{29}$Si value is approximately −99 ppm,[26,38] whereas we calculate a value of −95 ppm for the albite analog $Q^4$Si (Al,Na) molecule. The −96 ppm chemical shift for the $Q^3$Si (Al,Na) molecule is probably close to the true isotropic shift that would be observed experimentally as its value relative to the $Q^3$Si value of −98 ppm is consistent with, and of similar magnitude to, the observed deshielding of the $^{29}$Si nuclei as the number of Al next-nearest neighbors increase in aluminosilicate glasses, clays, and zeolites.[26,40−42]

**TABLE 3: Isotropic Chemical Shieldings $\sigma_{iso}$ and Chemical Shifts $\delta_{iso}$ for TMS and the $Q^n$ Si Molecules. Values are in ppm**

| | 6-31G* | | 6-31G(2d) | | 6-311+G** | | |
|---|---|---|---|---|---|---|---|
| molecule | $\sigma_{iso}$ | $\delta_{iso}$ | $\sigma_{iso}$ | $\delta_{iso}$ | $\sigma_{iso}$ | $\delta_{iso}$ | exptl |
| TMS[a] | 450 | | 432 | | 397 | | |
| $Q^2$Si | 529 | −79[b] | 507 | −75 | 484 | −87 | −91[c] |
| $Q^3$Si | 536 | −86 | 515 | −83 | 495 | −98 | −100[c] |
| $Q^3$Si (Al,Na) | 534 | −84 | 513 | −81 | 493 | −96 | |
| $Q^4$Si | 543 | −93 | 526 | −94 | 509 | −112 | −112[d] |
| $Q^4$Si (Al,Na) | 532 | −82 | 512 | −80 | 492 | −95 | −99[e] |
| $Q^4$Si (Al−$O_{br}$H) | 532 | −82 | 512 | −80 | 492 | −95 | |

[a] Additional calculations on TMS performed at 6-31G(3df,2p), $\sigma_{iso}$ = 419 ppm, and at 6-311+G(3df,2p), $\sigma_{iso}$ = 381 ppm. [b] Example calculation of $\delta_{iso}$: For the 6-31G* basis set, $\delta_{iso}$ of $Q^2$Si = ($\sigma_{iso}$ of TMS) − ($\sigma_{iso}$ of $Q^2$Si) = 450−529 = −79 ppm. [c] Reference 8. [d] References 8, 26, and 38. [e] References 38 and 43.

The GIAO calculations predict that protonation of the bridging oxygen (*i.e.*, Al−O−Si + $H^+ \rightarrow$ Al−($O_{br}$H)−Si) will result in no change in the experimental $^{29}$Si peak position because the $Q^4$Si (Al,Na) and $Q^4$Si (Al−$O_{br}$H) have the same isotropic chemical shifts. On the basis of the model proposed by Sykes and Kubicki,[3a] the GIAO results predict a 3 ppm increase in the chemical shift from −95 ppm ($Q^4$Si (Al,Na)) to −98 ppm ($Q^3$Si). This predicted shift in the peak maximum is in the opposite direction of the observed small to negligible experimental shift from −98.7 to −98.3 ppm.[6] However, because the GIAO calculations underestimate the $^{29}$Si chemical shift of albite by 4 ppm (−95 ppm for $Q^4$Si (Al,Na) *vs* −99 ppm from experiment), this discrepancy between theory and experiment is within the error limits of the calculations. Furthermore, isotropic chemical shifts of −98 and −100 ppm for the $Q^3$Si molecule and hydrous silica glass, respectively, are based on Al-free compositions. In anhydrous albite glass, $Q^4$Si have $n = 0-2$, that is, there are zero, one, or two Al next-nearest neighbors. If $Q^3$Si (*n*Al) are present in hydrous albite

**TABLE 4: Isotropic Chemical Shieldings $\sigma_{iso}$ and Chemical Shifts $\delta_{iso}$ for $Al^{3+}\cdot 6(H_2O)$ and $[Al(OH)_4]^{1-}\cdot 2(H_2O)$. Values are in ppm**

| | optimization basis | | | | | | | | |
|---|---|---|---|---|---|---|---|---|---|
| | | HF/3-21G** | | | HF/6-311+G** | | | MP2/6-311+G** | |
| NMR basis (HF/...) | $\sigma_{Al^{3+}}$ | $\sigma_{Al(OH)_4{}^{1-}}$ | $\delta_{Al(OH)_4{}^{1-}}$ | $\sigma_{Al^{3+}}$ | $\sigma_{Al(OH)_4{}^{1-}}$ | $\delta_{Al(OH)_4{}^{1-}}$ | $\sigma_{Al^{3+}}$ | $\sigma_{Al(OH)_4{}^{1-}}$ | $\delta_{Al(OH)_4{}^{1-}}$ |
| 3-21G** | 691 | 588 | 103[a] | 694 | 595 | 99 | 696 | 594 | 102 |
| 6-31G* | 633 | 555 | 78 | 636 | 560 | 76 | 638 | 558 | 80 |
| 6-31+G* | 631 | 558 | 73 | 631 | 562 | 69 | 633 | 562 | 71 |
| 6-31G(2d) | 622 | 550 | 72 | 625 | 556 | 69 | 626 | 554 | 72 |
| 6-311+G** | 612 | 526 | 86 | 614 | 531 | 83 | 615 | 531 | 84 |
| 6-311+G(3df,2p) | 610 | 524 | 86 | 613 | 529 | 84 | 614 | 529 | 85 |

[a] Example calculation of $\delta_{Al(OH)_4{}^{1-}}$: For the 3-21G** basis set, $\delta_{iso}$ of $Al(OH)_4{}^{1-}$ = ($\sigma_{iso}$ of $Al^{3+}\cdot 6(H_2O)$) − ($\sigma_{iso}$ of $Al(OH)_4{}^{1-}$) = 691 − 588 = 103 ppm.

glasses, then a consequence of the presence of Al nuclei in next-nearest neighbor sites and beyond will be some degree of deshielding of the Si nuclei from that considered using the Al-free model. As a result, hydrolysis of Al−O−Si linkages to form Al−OH and Si−OH should result in a predicted change in the $^{29}$Si peak maximum from −99 ppm (the experimental value for $Q^4$Si (Al, Na) in albite glass) to some value between −96 and −100 ppm where −96 ppm is the calculated value for the molecule $Q^3$Si (Al,Na) and −100 ppm is the experimental value for $Q^3$Si in hydrous silica glass. Thus, the water solubility mechanisms proposed by Kohn et al.,[1b] Pichavant et al.,[2] and Sykes and Kubicki[3a] are both consistent with the experimental $^{29}$Si NMR spectra.

**3.4. Al Isotropic Chemical Shieldings and Shifts.** In Table 4, Al isotropic chemical shieldings and chemical shifts are listed for the $Al^{3+}\cdot 6(H_2O)$ and $[Al(OH)_4]^{1-}\cdot 2(H_2O)$ clusters. Isotropic chemical shielding values appear to converge near 613 and 530 ppm for $Al^{3+}\cdot 6(H_2O)$ and $[Al(OH)_4]^{1-}\cdot 2(H_2O)$, respectively. Chemical shieldings predicted with 6-311+G** and 6-311+G(3df,2p) are similar regardless of the basis set which was used for molecular energy minimization. It is clear from Table 4 that the 3-21G** basis is not suitable for NMR shielding calculations, but molecular structures obtained with this basis set provide reasonable results compared to those obtained with HF/6-311+G** or MP2/6-311+G** calculations. This justifies our use of the 3-21G** basis set to obtain molecular structures for large aluminosilicate molecules provided larger basis sets are used to obtain the NMR parameters. The addition of a second set of d-functions lowers the chemical shielding (6-31G* vs 6-31G(2d)); however, the addition of extra d-functions does not affect the chemical shielding as much if the triply-split valence shell representation is used (6-311+G** *vs* 6-311+G(3df,2p)). The addition of the diffuse function to the 6-31G* basis does have a small impact of up to 5 ppm on the calculated chemical shieldings. Diffuse functions tend to move bond centers farther out from the central Al nucleus which results in a slightly greater electron density about the Al nucleus. Hence, the 6-31+G* chemical shieldings are larger (*i.e.*, more shielded) than the 6-31G* values.

Chemical shifts for the $[Al(OH)_4]^{1-}\cdot 2(H_2O)$ molecule calculated with the 6-31G*, 6-311+G**, and 6-311+G(3df,2p) basis sets are within ±6 ppm of the experimental value of 79.9 ppm for aqueous $[Al(OH)_4]^{1-}\cdot 2(H_2O)$. Although the 6-31G* absolute *chemical shieldings* are approximately 23−30 ppm larger than those obtained using either 6-311+G** or 6-311+G(3df,2p), the 6-31G* calculation predicts *relative chemical shifts* for the tetrahedral Al molecule nearest to the experimental value. Thus, compensating errors between basis set effects and neglect of solvation may result in fortuitously close agreement between the 6-31G* chemical shift and experiment. The chemical shifts based on the 3-21G** basis sets are significantly overestimated, whereas the 6-31+G* and 6-31G(2d) chemical shifts are significantly underestimated.

**TABLE 5: Isotropic Chemical Shieldings $\sigma_{iso}$ and Chemical Shifts $\delta_{iso}$ for the $Q^n$ Al Molecules. Values are in ppm**

| | 6-31G* | | 6-31G(2d) | | 6-311+G** | |
|---|---|---|---|---|---|---|
| molecule | $\sigma_{iso}$ | $\delta_{iso}$ | $\sigma_{iso}$ | $\delta_{iso}$ | $\sigma_{iso}$ | $\delta_{iso}$ |
| $Al^{3+}\cdot 6(H_2O)$ | 633 | | 622 | | 612 | |
| $Q^3$Al (Na) | 576 | 57[a] | 573 | 49 | 548 | 64 |
| $Q^4$Al (Na) | 572 | 61 | 570 | 52 | 545 | 67 |
| $Q^4$Al (Al,Na) | 568 | 65 | 566 | 56 | 542 | 70 |
| $Q^4$Al ($O_{br}$H) | 576 | 57 | 571 | 51 | 546 | 66 |
| $Q^3$Al | 569 | 64 | | | | |
| $Q^4$Al | 569 | 64 | | | | |

[a] Example calculation of $\delta_{iso}$: For the 6-31G* basis set, $\delta_{iso}$ of $Q^3$Al (Na) = ($\sigma_{iso}$ of $Al^{3+}\cdot 6(H_2O)$) − ($\sigma_{iso}$ of $Q^3$Al (Na)) = 633−576 = 57 ppm.

Absolute chemical-shielding values for the aluminosilicate molecules decrease with increasing basis size for the same optimized structure. Chemical shifts typically change by less than 10 ppm as a function of basis set for a given molecule. The exceptions are chemical shifts based on the 6-31G(2d) shielding values for which the chemical shifts appear to be significantly underestimated. The isotropic chemical shift for crystalline albite is 63.4 ppm[38,43] and our value for the model albite structure $Q^4$Al (Na), is 61 ppm at 6-31G* and 67 ppm at 6-311+G** (Table 5). $^{27}$Al isotropic chemical shifts have not been determined for hydrous or anhydrous albite composition glasses. In general, crystals and their isochemical glasses do not necessarily have identical chemical shifts. For example, quartz has a $^{29}$Si chemical shift of −107 ppm and silica glass has a value of −112 ppm.[26,44] It is not clear whether Al in albite would be more shielded or less than Al in glass of albite composition, but the isotropic values are not expected to be significantly different in either case. The $^{27}$Al peak maximum for the 500 MHz spectrum of albite glass is at 55 ppm[43] and probably near the true isotropic chemical shift for Al in this composition glass. In addition, line shape simulations of NMR spectra generated at 500 MHz for an aluminosilicate glass composition slightly more Si rich than albite calculate a $^{27}$Al $\delta_{iso}$ of approximately 60 ppm.[45] For all basis sets (Table 5), the $Q^3$Al (Na) molecule has a smaller isotropic chemical shift than the $Q^4$Al (Na) and has the same or similar shift as that calculated for $Q^4$Al ($O_{br}$H).

At 360 MHz, the $^{27}$Al peak maximum in dry albite glass is 50.5 ppm. With increasing water concentration, the peak maximum shifts to 53 ppm and the line width narrows approximately 2.5 ppm.[1a] At 400 MHz, the peak maximum at 53 ppm shifts approximately 1 ppm to 54 ppm and the line width narrows by 3 ppm.[6] Based on this data, Kohn et al.[1a] suggested that hydrolysis of Al−O−Si linkages to form Al−(OH) and Si−(OH) terminal bonds (*i.e.*, $Q^4 \rightarrow Q^3$) did not occur.

Instead, they proposed exchange of $H^+$ for $Na^+$ at the charge-balance sites as the principal water solubility mechanism in aluminosilicate compositions. Kohn et al.[1b] and Pichavant et al.[2] revised the model to include protonation of the bridging oxygens (*i.e.*, $O_{br}$−H bond order = 1) analogous to the protonated Si−O−Al linkages in acid zeolites *via* the reaction $Al-O-Si + H^+ \rightarrow Si-(O_{br}H)-Al$ as opposed to simple exchange of $H^+$ for $Na^+$ in charge-balancing sites. The above studies discounted the presence of $Q^3Al$ sites with terminal −(OH) groups because it was assumed that the QCC of a $Q^3Al$ site was greater than the QCC for a $Q^4Al$ site based on comparisons with $^{27}Al$ QCCs in crystalline calcium aluminates.[46] Thus, the $^{27}Al$ NMR spectra of hydrous albite glass would have a broader, not narrower, peak if $Q^3Al$ (OH) were present. In addition, the 2.5 ppm shift in the $^{27}Al$ peak maximum between anhydrous (50.5 ppm) and hydrous glasses (53 ppm) was deemed inconsistent with the 70 ppm peak maximum observed for $Q^3Al$ sites in crystalline phyllosilicates[40] for which the one nonbridging oxygen is bonded to an octahedral metal cation.

In contrast, Sykes and Kubicki[3ab] interpreted the NMR and vibrational spectra of hydrous aluminosilicate glasses to be consistent with the presence of $Q^3Al$ sites with terminal −(OH) groups. They assumed that the isotropic chemical shift of a $Q^3Al$ is not likely to be near 70 ppm as observed in crystalline phyllosilicates because terminal T−(OH) bonds are very different from T−(OM) bonds (where M = an octahedral metal cation). Further, $Q^3Si$ (OH) species have isotropic chemical shifts near −100 ppm[8] (a shift of 12 ppm from $Q^4Si$) as opposed to $Q^3Si$ (OM) sites which have isotropic chemical shifts near −90 ppm[37,38] (a shift of approximately 22 ppm from $Q^4Si$). Sykes and Kubicki[3a] also assumed that $Q^3Al$ nuclei would have smaller QCCs than $Q^4Al$ because the flexible terminal Al−(OH) bond permits greater relaxation of the electronic environment around the Al nuclei. The water solubility mechanism proposed by Sykes and Kubicki[3a] assumes that a $Q^3Al$ species with a terminal −(OH) group has a smaller QCC and similar but slightly larger isotropic chemical shift than a $Q^4Al$ species.

The GIAO calculations on the model $Q^3$ and $Q^4Al$ molecules indicate that both $Q^3Al$ nuclei and $Q^4Al$ ($O_{br}H$) have similar isotropic chemical shifts to $Q^4Al$ nuclei (Table 5). Therefore, the results are not consistent with the assumption made by Kohn et al.[1ab] that $Q^3Al$ sites have isotropic chemical shifts approximately 15+ ppm more deshielded than $Q^4Al$ nuclei.

**3.5. Al Quadrupolar Coupling Constants.** $^{27}Al$ peak maxima are more shielded from the theoretical and experimental isotropic shifts due to the interaction of the nuclear quadrupole moment with the electric field gradient (EFG)

$$\delta_{peak} = \delta_{iso} - \delta_{qs} \qquad (1)$$

where $\delta_{peak}$ is the observed peak, $\delta_{iso}$ is the isotropic chemical shift, and $\delta_{qs}$ is the quadrupolar shift. $\delta_{peak}$ is directly observable in the experimental spectra, and $\delta_{iso}$ is what we directly calculate. Thus, to compare our calculations directly with experimental spectra, an estimate of $\delta_{qs}$ either from experiment or theory is necessary. $\delta_{qs}$ can be calculated from the quadrupolar coupling constants (QCC; see Methods section) using the following equation:

$$\delta_{qs} = -\frac{3}{40}\frac{\mathrm{QCC}^2}{\omega_L{}^2}\frac{I(I+1) - 9m(m-1) - 3}{I^2(2I-1)^2}\left(1 + \frac{\eta^2}{3}\right) \qquad (2)$$

where $\omega_L$ = Larmor frequency of the nuclei, $I$ = the spin state, and $m$ = the z-quantum number of the ($m$, $m-1$) transition. Table 6 lists the Al QCCs calculated for the aluminosilicate molecules and the predicted quadrupolar shifts of the peak maxima assuming an ambient magnetic field strength of 400 MHz. The calculated quadrupolar shifts appear too large and indicate that our calculations overestimate QCC values for these molecules. Kirkpatrick et al.[43] and Phillips et al.[47] report Al QCCs of 3.23 to 3.29 MHz for crystalline low albite and microcline, respectively. Our values are two−three times larger than those cited for the minerals. It is uncertain whether smaller or larger QCCs are expected in the minerals or isochemical glasses, but it is unlikely that QCCs would vary by a factor of 2 to 3 between crystal and glass because the local structure in the glass is thought to be similar to that in the crystal. Indeed, an Al QCC of 3.9 MHz has been reported for the glass composition, $NaAlSi_{5.3}O_{12.6}$, which is close to that of albite, $NaAlSi_3O_8$.[45]

**TABLE 6: Quadrupolar Coupling Constants QCC and Corresponding Quadrupolar Shifts $\delta_{qs}$. Values are in MHz and ppm, Respectively**

| | 6-31G* | | 6-31G(2d) | | 6-311G** | |
|---|---|---|---|---|---|---|
| molecule | QCC | $\delta_{qs}$ | QCC | $\delta_{qs}$ | QCC | $\delta_{qs}$ |
| $Q^3Al$ (Na) | 6.105 | 21 | 6.265 | 22 | 7.337 | 30 |
| $Q^4Al$ (Na) | 8.410 | 39 | 8.974 | 45 | 10.930 | 66 |
| $Q^4Al$ (Al,Na) | 8.875 | 44 | 9.607 | 51 | 11.812 | 77 |
| $Q^4Al$ ($O_{br}H$) | 15.772 | 138 | 15.161 | 127 | 18.880 | 197 |

Although our calculations may overestimate the QCC values, relative differences in Al QCC values between molecules may be more internally consistent. For example, for all basis sets, Al QCC values for the $Q^3Al$ (Na) molecule are approximately 70% of the values for Al in the $Q^4Al$ (Na) molecule; $Q^4Al$ (Na) values are approximately 94% of the values in $Q^4Al$ (Al,Na), and 55% of the values in $Q^4Al$ ($O_{br}H$). Thus we may be able to estimate the relative magnitudes of quadrupolar shifts and directional shifts in the peak maxima in $^{27}Al$ NMR spectra.

The QCC values determined from the EFG tensors predict quadrupolar shifts of 21 ppm or more and would result in significant broadening of the line shapes (Table 6). If true, peak maxima in the $^{27}Al$ NMR spectra of aluminosilicate glass compositions would be closer to 30 ppm or less; the absolute values of the QCCs are clearly in error. However, we can calculate QCC values using eqs 1 and 2, the experimental peak maxima, and the GIAO-predicted isotropic chemical shifts. As a basis for future discussion, QCC values calculated using the EFG data will be designated as Method 1 and QCC values calculated using eqs 1−6, the experimental peak maxima, and the GIAO-predicted isotropic chemical shifts will be designated Method 2.

From eqs 1 and 2, the QCC for the $Q^4Al$ (Na) nuclei is 3.568 MHz based on a $^{27}Al$ $\delta_{peak} = 53$ ppm for albite glass at 400 MHz[6] and a $\delta_{iso} = 61$ ppm (6-31G*; Table 5). A similar QCC value of 3.867 MHz is obtained using a $^{27}Al$ $\delta_{peak} = 55$ ppm for albite glass at 500 MHz[43] and $\delta_{iso} = 61$ ppm. The predicted QCC values, based on eqs 1 and 2 and the GIAO isotropic chemical shifts, are in the range of reported $^{27}Al$ QCC values of 3.23 to 3.29 MHz for crystalline low albite and microcline[43,47] and 3.9 MHz for a sodium aluminosilicate glass close to the albite composition.[45] Because of the similarity of the calculated QCC values to each other and to the experimental values using peak maxima obtained at two different magnetic field strengths from two different studies and our $\delta_{iso}$ results, we are confident that the QCC values obtained from eqs 1 and 2 and our GIAO calculations (*i.e.*, Method 2) are accurate.

The above calculation assumes that only $Q^4Al$ (Na) nuclei contribute to the $^{27}Al$ NMR signal in aluminosilicate glasses. However, it is known that some fraction (0.25−0.50) of the $Q^4Al$ nuclei have Al next-nearest neighbors (*i.e.*, $Q^4Al$ (Al,Na) sites are present in aluminosilicate glasses and in hightemperature annealed feldspars[3c,41,48]). As a consequence, eq 1 is rewritten in terms of two chemically distinct Al sites

$$\delta_{peak} = x(\delta_{iso}x - \delta_{qs}{}^{x}) + y(\delta_{iso}{}^{y} - \delta_{qs}{}^{y}) \tag{3}$$

where $x$ equals the fraction of $Q^4$Al and $y$ equals the fraction of $Q^4$Al (Al,Na) in the aluminosilicate glass ($x + y = 1$). Using the appropriate $\delta_{iso}$ values from Table 5 (6-31G*) and $\delta_{peak} =$ 53 ppm and setting $y = 0.25$ (*i.e.*, the minimum for Al−O−Al bonding at the albite composition), eq 3 reduces to

$$9 = 0.75(\delta_{qs}{}^{x}) + 0.25(\delta_{qs}{}^{y}) \tag{4}$$

The QCC values for $Q^4$Al (Na) and $Q^4$Al (Al,Na) can be obtained by iteration of eqs 2 and 4. The calculated QCC values are 3.785 and 3.929 MHz for the $Q^4$Al (Na) and $Q^4$Al (Al,Na) nuclei, respectively. If we set $y = 0.50$, the calculated QCC values are 3.785 and 4.121 MHz, respectively. The ratio of the QCC values obtained by solving eqs 2 and 4, 0.963 for $y = 0.25$ and 0.918 for $y = 0.50$, are very similar to and bracket the ratio of the QCC values for these two molecules calculated from Method 1, 0.948. Therefore, the relative differences in Al QCC values between molecules calculated from the EFG data (Method 1) appear to be accurate, although the absolute magnitudes are overestimated. If true, then the Al QCC value for the $Q^3$Al (Na) molecule can be obtained from the following equality

$$\left[\frac{\mathrm{QCC}^{Q^3\mathrm{Al\ (Na)}}}{\mathrm{QCC}^{Q^4\mathrm{Al\ (Na)}}}\right]_{\mathrm{Method\ 2}} = \left[\frac{\mathrm{QCC}^{Q^3\mathrm{Al\ (Na)}}}{\mathrm{QCC}^{Q^4\mathrm{Al\ (Na)}}}\right]_{\mathrm{Method\ 1}} \Rightarrow \frac{\mathrm{QCC}^{Q^3\mathrm{Al\ (Na)}}}{3.785} = \frac{6.105}{8.410} \tag{5}$$

for which we obtain a value of 2.748 MHz.

Using equations 2 and 3, we can predict the $^{27}$Al peak maximum of hydrous albite glass by assuming that water preferentially reacts with the $Q^4$Al (Al,Na) species, *i.e.*, Al−O−Al → Al−OH. For this case, $y$ equals the fraction of $Q^3$Al (Na) in the aluminosilicate glass. Using the appropriate QCC values and isotropic chemical shifts, we calculate $\delta_{peak} = 52.1$ ppm for $y = 0.25$ and 52.2 ppm for $y = 0.5$. The calculations predict that the peak maximum should shift by approximately 1 ppm from 53 to 52 ppm between anhydrous and hydrous albite compositions. This result is quite consistent with the observed shift from 53 to 54 ppm given that the QCC values are estimates and the difficulty in precisely identifying experimental $^{27}$Al peak maxima.

Alternatively, we can predict the $^{27}$Al peak maximum of hydrous albite glass assuming that water interacts equally with $Q^4$Al (Na) (*i.e.*, Al−O−Si → Al,Si−OH) and $Q^4$Al (Al,Na) species:

$$\delta_{peak} = x'[x(\delta_{iso}{}^{x} - \delta_{qs}{}^{x}) + y(\delta_{iso}{}^{y} - \delta_{qs}{}^{y})] + z(\delta_{iso}{}^{z} - \delta_{qs}{}^{z}) \tag{6}$$

where $x'$ is the fraction of Al in all $Q^4$ sites and $x$ and $y$ are the fractions of Al in $Q^4$Al (Na) and $Q^4$Al (Al,Na) sites, respectively; $x + y = 1$; $z$ equals the fraction of Al in $Q^3$Al (Na) sites; $x' + z = 1$; and all other variables are as indicated before. For either $y = 0.25$ or 0.50 and setting $x = z$, we obtain a $\delta_{peak}$ of 52.7 ppm. Our results predict essentially no change in the peak maximum and are in agreement within error of the measured peak maxima.

We have also calculated the shift in the peak maximum if the water solubility mechanism occurred by the protonation of bridging oxygens, Al−O−Si → Al−($O_{br}$H)−Si. The Al QCC for the $Q^4$Al ($O_{br}$H) molecule is 7.099 MHz using an equality similar to eq 5:

$$\left[\frac{\mathrm{QCC}^{Q^4\mathrm{Al\ (O_{br}H)}}}{\mathrm{QCC}^{Q^4\mathrm{Al\ (Na)}}}\right]_{\mathrm{Method\ 2}} = \left[\frac{\mathrm{QCC}^{Q^4\mathrm{Al\ (O_{br}H)}}}{\mathrm{QCC}^{Q^4\mathrm{Al\ (Na)}}}\right]_{\mathrm{Method\ 1}} \Rightarrow \frac{\mathrm{QCC}^{Q^4\mathrm{Al\ (O_{br}H)}}}{3.785} = \frac{15.772}{8.410} \tag{7}$$

The calculations are performed as before using eqs 3 and 6 but substituting the appropriate values for $Q^4$Al ($O_{br}$H) in place of $Q^3$Al (Na). For $y = 0.25$, we calculate peak maxima near 46 ppm for either equation. If the above calculations are correct, then protonation of the bridging oxygen is not a viable water solubility mechanism as the calculated shift in the peak maximum (53 → 46 ppm) is outside the error in our calculations and the large QCC of the Al nuclei in $Q^4$Al ($O_{br}$H) sites would result in significantly broader line widths, neither of which are observed.

## 4. Conclusions

In the present study, we have found that molecular orbital calculations on large aluminosilicate clusters can accurately predict experimentally observed trends in the NMR spectra of aluminosilicate glasses. Isotropic chemical shifts, relative to TMS, calculated for the $Q^2$Si (−87 ppm), $Q^3$Si (−98 ppm), and the $Q^4$Si (−112 ppm) using 6-311+G** (Table 3) are comparable to the experimental values of −91 ppm, −100 ppm, and −112 ppm, respectively. Isotropic chemical shifts for the $[Al(OH)_4]^{1-}\cdot 2(H_2O)$ molecule calculated with the 6-31G*, 6-311+G**, and 6-311+G(3df,2p) basis sets are within ±6 ppm of the experimental value of 79.9 ppm for aqueous $[Al(OH)_4]^{1-}\cdot 2(H_2O)$.

The calculations predict that protonation of the bridging oxygen (*i.e.*, Al−O−Si + $H^+$ → Al−($O_{br}$H)−Si) will result in no change in the experimental $^{29}$Si peak position because the $Q^4$Si (Al,Na) and $Q^4$Si (Al−$O_{br}$H) have the same isotropic chemical shifts and hydrolysis of Al−O−Si linkages to form Al−OH and Si−OH would shift the $^{29}$Si peak maximum from −99 ppm (the experimental value for $Q^4$Si (Al,Na) in albite glass) to some value between −96 and −100 ppm. Calculations on the model $Q^3$ and $Q^4$Al molecules indicate that both $Q^3$Al nuclei and $Q^4$Al ($O_{br}$H) have similar Al isotropic chemical shifts to $Q^4$Al nuclei; however, the large QCC of the Al nuclei in $Q^4$Al ($O_{br}$H) sites would result in significantly broader $^{27}$Al line widths and a calculated shift difference between the Al isotropic chemical shift and the Al observed peak maximum (53 → 46 ppm) outside the error of the calculations, neither of which are observed in the experimental spectra.

**Acknowledgment.** D.S. and T.C.F. acknowledge support from NSF Grant CHE9500735. J.D.K. acknowledges support from O.N.R. and O.N.T. Computational facilities were provided by the Department of Defense HPC initiative on the Cray C-90 at CEWES and the Convex Exemplar at NCCOSC.

## References and Notes

(1) (a) Kohn, S. C.; Dupree, R.; Smith, M. E. *Geochim. Cosmochim. Acta* **1989**, *53*, 2925. (b) Kohn, S. C.; Dupree, R.; Mortuza, M. G. *Chem. Geol.* **1992**, *96*, 399. (c) Kohn, S. C.; Smith, M. E.; Dupree, R. *Geochem. Cosmochem. Acta* **1994**, *58*, 1377.

(2) Pichavant, M.; Holtz, F.; McMillan, P. F. *Chem. Geol.* **1992**, *96*, 303.

(3) (a) Sykes, D.; Kubicki, J. D. *Geochim. Cosmochim. Acta* **1993**, *57*, 1039. (b) Sykes, D.; Kubicki, J. D. *Geochim. Cosmochim. Acta* **1994**, *58*, 1381. (c) Kubicki, J. D.; Sykes, D. *Geochim. Cosmochim. Acta* **1995**, *59*, 4791.

(4) Mysen, B. O.; Virgo, D.; Harrison, W.; Scarfe, C. M. *Am. Mineral*. **1980**, *65*, 900.

(5) Mysen, B. O.; Virgo, D. *Chem. Geol*. **1986**, *57*, 333.

(6) Sykes, D.; Sato, R.; Luth, R. W.; McMillan, P. F.; Poe, B. *Geochim. Cosmochim. Acta* **1993**, *57*, 3575.

(7) Kubicki, J. D.; Blake, G. A.; Apitz, S. E. *Geochim. Cosmochim. Acta* **1996**, *60*, 4897.

(8) Farnan, I.; Kohn, S. C.; Dupree, R. *Geochim. Cosmochim. Acta* **1987**, *51*, 2869.

(9) Jameson, C. J.; Jameson, A. K. *Chem. Phys. Lett*. **1988**, *149*, 300.

(10) Kutzelnigg, W.; Fleischer, M.; Schindler, M. In *NMR 23. Deuterium and Shift Calculation*; Diehl, P., et al., Eds.; Springer-Verlag: Berlin, 1991; p 165.

(11) Wolff, R.; Radeglia, R. *J. Mol. Struct. (THEOCHEM)* **1994**, *313*, 111.

(12) Frisch, M. J.; Trucks, G. W.; Schlegel, H. B.; Gill, P. M. W.; Johnson, B. G.; Robb, M. A.; Cheeseman, J. R.; Keith, T.; Petersson, G. A.; Montgomery, J. A.; Raghavachari, K.; Al-Laham, M. A.; Zakrzewski, V. G.; Ortiz, J. V.; Foresman, J. B.; Cioslowski, J.; Stefanov, B. B.; Nanayakkara, A.; Challacombe, M.; Peng, C. Y.; Ayala, P. Y.; Chen, W.; Wong, M. W.; Andres, J. L.; Replogle, E. S.; Gomperts, R.; Martin, R. L.; Fox, D. J.; Binkley, J. S.; Defrees, D. J.; Baker, J.; Stewart, J. P.; Head-Gordon, M.; Gonzalez, C.; Pople, J. A. *Gaussian 94*, Revision C.3; Gaussian, Inc.: Pittsburgh, 1995.

(13) Peng, C. Y.; Ayala, P. Y.; Schlegel, H. B.; Frisch, M. J. *J. Comput. Chem*. **1995**, *17*, 49.

(14) Frisch, M. J.; Head-Gordon, M.; Pople, J. A. *Chem. Phys. Lett*. **1990**, *166*, 275.

(15) Schlegel, H. B. *J. Comput. Chem*. **1982**, *3*, 214.

(16) Wolinski, K.; Hinton, J. F.; Pulay, P. *J. Am. Chem. Soc*. **1990**, *112*, 8251.

(17) London, F. J. *Phys. Radium* **1937**, *8*, 397.

(18) McWeeny, R. *Phys. Rev*. **1962**, *126*, 1028.

(19) Ditchfield, R. *Mol. Phys*. **1974**, *27*, 789.

(20) Dodds, J. L.; McWeeny, R.; Sadlej, A. L. *Mol. Phys*. **1980**, *41*, 1419.

(21) Sheedan, W. F.; Shomaker, V. *J. Am. Chem. Soc*. **1952**, *74*, 3956.

(22) Beagley, B.; Monaghan, J. J.; Hewitt, T. G. *J. Mol. Struct. (THEOCHEM)* **1971**, *8*, 395.

(23) Shannon, R. D.; Prewitt, C. T. *Acta Crystallogr*. **1969**, B25, 925.

(24) Wainwright, J. E.; Starkey, J. *Z. Kristallogr*. **1971**, *133*, 75.

(25) Kroll, H.; Ribbe, P. H. In *Reviews in Mineralogy*. Part 2 (Feldspar Mineralogy); Ribbe, P. H., Ed.; The Mineralogical Society of America: Washington, DC, 1983; p 57.

(26) Oestrike, R.; Yang, W. H.; Kirkpatrick, R. J.; Hervig, R. L.; Navrotsky, A.; Montez, B. *Geochim. Cosmochim. Acta* **1987**, *51*, 2199.

(27) Lasaga, A. C.; Gibbs, G. V. *Phys. Chem. Miner*. **1988**, *16*, 29.

(28) (a) Hill, J.-R.; Sauer, J. *Z. Phys. Chem*. **1989**, *270*, S. 203. (b) Hill, J.-R.; Sauer, J. *J. Phys. Chem*. **1994**, *98*, 1238.

(29) Bartsch, M.; Bornhauser, P.; Calzaferri, G.; Imhof, R. *J. Phys. Chem*. **1994**, *98*, 2817.

(30) Kubicki, J. D.; Sykes, D. *Geochim. Cosmochim. Acta* **1995**, *59*, 4791.

(31) Mozzi, R. L.; Warren, B. E. *J. Appl. Crystallogr*. **1969**, *2*, 164.

(32) Geisinger, K. L.; Gibbs, G. V.; Navrotsky, A. *Phys. Chem. Miner*. **1985**, *11*, 266.

(33) Wong, J.; Angell, C. A. *Glass Structure by Spectroscopy*; Marcel Dekker, Inc.: New York, 1976.

(34) Ross, N. L.; Shu, J. F.; Hazen, R. M.; Gasparik, T. *Am. Mineral*. **1990**, *75*, 739.

(35) Wyekoff, R. W. G. *Crystal Structures*; Intersciences Publishers: New York, 1978.

(36) Fleischer, U.; Schindler, M.; Kutzelnigg, W. *J. Chem. Phys*. **1987**, *86*, 6337.

(37) Dupree, R.; Holland, D.; McMillan, P. W.; Pettifer, R. F. *J. Non-Cryst. Solids* **1984**, *68*, 399.

(38) Murdoch, J. B.; Stebbins, J. F.; Carmichael, I. S. E. *Am. Mineral*. **1985**, *70*, 332.

(39) Oestrike, R.; Kirkpatrick, R. J. *Am. Mineral*. **1988**, *73*, 534.

(40) Kinsey, R. A.; Kirkpatrick, R. J.; Hower, J.; Smith, K. A.; Oldfield, E. *Am. Mineral*. **1985**, *70*, 537.

(41) Yang, W.-H.; Kirkpatrick, R. J.; Henderson, D. M. *Am. Mineral*. **1986**, *71*, 712.

(42) Lippmaa, E.; Samoson, A.; Magi, M. *J. Am. Chem. Soc*. **1986**, *108*, 1730.

(43) Kirkpatrick, R. J.; Kinsey, R. A.; Smith, K. A.; Henderson, D. M.; Oldfield, E. *Am. Mineral*. **1985**, *70*, 106.

(44) Smith, J. V.; Blackwell, C. S. *Nature* **1983**, *303*, 223.

(45) Dirken, P. J.; Nachtegaal, G. H.; Kentgens, A. P. M. Solid State *Nucl. Magn. Reson*. **1995**, *5*, 189.

(46) Müller, D.; Gessner, W.; Behrens, H.; Scheler, G. *Chem. Phys. Lett*. **1981**, *79*, 59.

(47) Phillips, B. L.; Kirkpatrick, R. J.; Hovis, G. L. *Phys. Chem. Miner*. **1988**, *16*, 262.

(48) Kubicki, J. D.; Sykes, D. *Phys. Chem. Miner*. **1993**, *19*, 381.